

Performance Evaluation of Ammonia Refrigeration Systems in a Texturizing Plant

Abdul Cholik^{1,*}, Nanang Ruhyat^{1,*} and Sentot Novianto²

¹Department of Mechanical Engineering, Universitas Mercu Buana, Meruya Selatan, Jakarta 11680, Indonesia

²Department of Mechanical Engineering, Universitas Trisakti, Petamburan, Jakarta 11440, Indonesia

*Corresponding Authors: abdulcholik766@gmail.com (AC), nanang.ruhyat@mercubuana.ac.id (NR)

Abstract

This study evaluates the performance of an ammonia refrigeration system used as a cooling medium in a texturizing plant. The analysis was conducted over a 10-day period, focusing on key performance indicators such as compressor work, condenser exhaust heat, refrigeration effect, mass flow rate, Coefficient of Performance (COP), and overall system efficiency. The data revealed that the system performed optimally on Day 5, achieving a peak efficiency of 91%, with compressor work at 304.1 kJ/kg and condenser exhaust heat at 1414.6 kJ/kg. In contrast, the lowest efficiency was recorded on Day 3, at 77%. The refrigeration effect reached its highest value of 491.3 kJ/kg on Day 3, highlighting efficient heat absorption despite lower overall system efficiency. On Day 4, the mass flow rate was 0.001049929 kg/s, with an actual COP of 1.39, while the ideal COP peaked on Day 10 at 1.69, reflecting the system's theoretical maximum efficiency under optimal conditions. The study emphasizes the critical role of the condenser in the system's performance. Optimizing the condenser's operation by controlling temperature, pressure, and flow rates, alongside regular maintenance, significantly impacts system efficiency. The findings suggest that careful monitoring of operational parameters, including compressor work and refrigerant flow, can enhance the overall efficiency and reliability of ammonia refrigeration systems in industrial settings. This research provides practical insights into improving the cooling performance, reducing energy consumption, and ensuring consistent production quality in texturizing plants.

Article Info:

Received: 3 June 2024

Revised: 9 September 2024

Accepted: 13 September 2024

Available online: 9 October 2024

Keywords:

Ammonia refrigeration system; texturizing plant cooling; compressor work efficiency; condenser performance; coefficient of performance

© 2024 The Author(s). Published by Universitas Mercu Buana (Indonesia). This is an open-access article under [CC BY-SA](https://creativecommons.org/licenses/by-sa/4.0/) License.



1. Introduction

Ammonia-based refrigeration systems, particularly using ammonia (R717), are extensively utilized in industrial applications such as chemical processing, cold storage, and textile production due to their favorable thermodynamic properties, energy efficiency, and environmental benefits. Ammonia is characterized by its high heat absorption capacity, zero ozone depletion potential (ODP), and zero global warming potential (GWP), making it an attractive refrigerant choice in large-scale refrigeration systems [1]. The efficiency of ammonia refrigeration systems is critical in industrial settings, especially in processes like texturizing, where maintaining optimal cooling is essential for product quality and energy consumption [2].

Despite the advantages of ammonia as a refrigerant, challenges persist in optimizing the performance of these systems. One significant issue is maintaining high efficiency under varying operational loads and external conditions. Research indicates that the performance of ammonia refrigeration systems can be influenced by factors such as system design, operational parameters, and external environmental conditions [3], [4]. For instance, the integration of advanced control systems can enhance the stability of temperature and pressure within the refrigeration cycle, thereby improving overall system efficiency [2]. Moreover, the implementation of hybrid systems that combine mechanical compression with thermochemical storage of ammonia vapor has shown promise in enhancing cooling performance while optimizing energy use [5].

The performance of ammonia refrigeration systems has been a focal point of research in various industrial applications, particularly in cold storage and chemical processing plants. Notably, studies by Zhao et al. [1] have contributed valuable insights into the coefficient of performance (COP) and

How to cite:

A. Cholik, N. Ruhyat, and S. Novianto, "Performance evaluation of ammonia refrigeration systems in a texturizing plant," *Int. J. Innov. Mech. Eng. Adv. Mater.*, vol. 6, no. 3, pp. 161-172, 2024

energy consumption of these systems. However, these studies have not sufficiently addressed the performance of ammonia refrigeration systems in high-temperature industrial environments, such as texturizing plants, where efficient cooling is crucial for maintaining product quality [6].

Ammonia (R717) is favored in industrial refrigeration due to its excellent thermodynamic properties, including high heat absorption capacity and energy efficiency. It is also recognized for its environmental benefits, having zero ozone depletion potential (ODP) and zero global warming potential (GWP) [7], [8]. The studies conducted by Zhao et al. [1] highlight the significance of maintaining optimal refrigeration conditions to ensure product integrity, especially in processes sensitive to temperature fluctuations. Furthermore, the research indicates that while ammonia systems are prevalent in large-scale refrigeration, their performance under varying operational loads and external conditions remains a challenge that requires further investigation [9].

In high-temperature environments, such as texturizing plants, the efficiency of ammonia refrigeration systems can be significantly impacted by external heat loads. This necessitates the development of advanced control strategies and system designs that can adapt to fluctuating conditions. For instance, hybrid systems that integrate mechanical compression with thermochemical storage of ammonia vapor have shown promise in enhancing cooling performance while optimizing energy consumption [10]. Additionally, the implementation of vapor injection techniques has been suggested as a method to improve the COP of ammonia refrigeration systems, particularly in scenarios where cooling demands vary [11].

Current research on ammonia refrigeration systems predominantly emphasizes performance analysis in controlled environments, often neglecting the complexities of industrial settings where operational conditions can fluctuate significantly. This gap is particularly evident in studies that focus on overall system efficiency, which frequently overlook the critical role of the condenser in driving performance. For instance, while studies such as those by Kazemiani-Najafabadi et al. [12] have explored the optimization of ammonia-water combined systems, they primarily address theoretical models without delving into the practical implications of condenser performance in dynamic industrial environments.

This study presents an approach by evaluating the performance of an ammonia refrigeration system in an industrial texturizing plant over a 10-day period. The research focuses specifically on the dynamic interaction between compressor work, condenser exhaust heat, and system efficiency under fluctuating operating conditions. Unlike previous studies, this research highlights the critical role of the condenser in optimizing system performance and provides actionable insights for improving system efficiency through temperature and pressure control, flow optimization, and regular maintenance. The primary objective of this research is to evaluate the performance of the ammonia refrigeration system used in the texturizing plant by analyzing key parameters such as compressor work, condenser exhaust heat, refrigeration effect, mass flow rate, and COP. The study aims to identify the factors that most significantly influence system efficiency and to provide recommendations for optimizing the condenser's performance to improve overall system reliability and energy efficiency.

2. Methods

2.1. Research stages

This research was conducted in several stages, as outlined in the flowchart in Figure 1. The process begins with an extensive literature review aimed at summarizing previous studies on the performance analysis of ammonia refrigeration systems. Following this, the research problem is formulated by identifying key issues related to the ammonia refrigeration system, specifically in the context of the texturizing plant for palm oil process in Serang, Indonesia.

The data collection phase involves measuring various operational parameters of the condenser, including inlet and outlet temperatures, compressor work, and exhaust heat. The ammonia refrigeration system used in this study employs R-717, a refrigerant widely utilized in industrial refrigeration systems due to its excellent thermodynamic properties, high energy efficiency, and environmentally friendly characteristics. R-717 is particularly valued for its zero-ozone depletion potential (ODP) and a global warming potential (GWP) of zero, as shown in Figure 2.

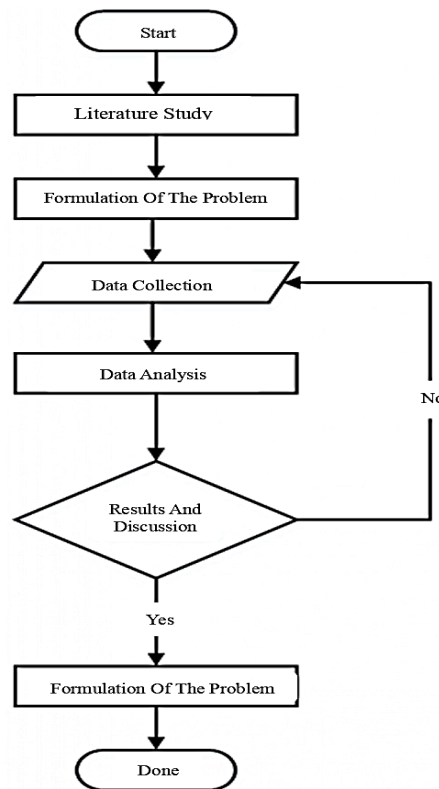


Figure 1. Flow chart of the research

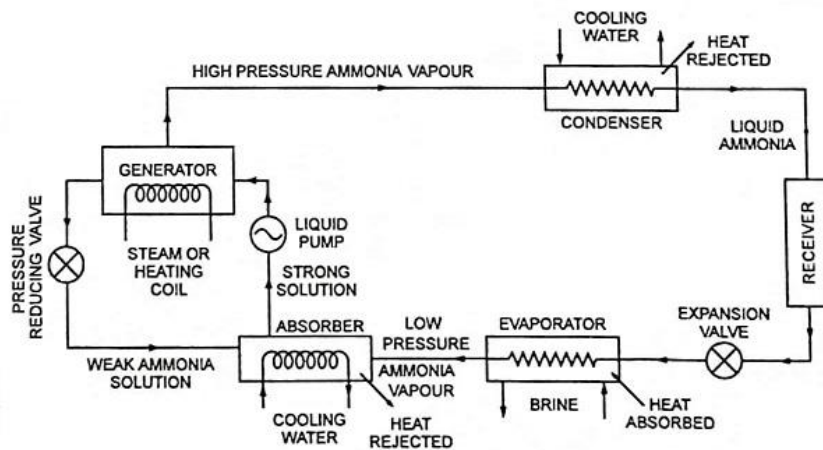


Figure 2. Ammonia refrigeration cycle

The vapor compression refrigeration cycle shown in Figure 2. The cycle consists of four primary operational phases: compression, condensation, expansion, and evaporation. The cycle begins with the compressor, where the refrigerant, in the form of saturated vapor, is drawn from the evaporator. The compressor increases the pressure and temperature of the refrigerant by compressing it into a high-pressure, high-temperature vapor [6]. The high-pressure vapor then flows into the condenser, where it releases heat to the surrounding environment. This heat transfer occurs as the vapor cools and condenses into a liquid state. The refrigerant exits the condenser as a saturated liquid, ready for the next phase of the cycle [13]. After leaving the condenser, the refrigerant passes through the expansion valve, where its pressure is significantly reduced. This pressure drop causes the refrigerant to expand and cool rapidly. The refrigerant, now in a low-pressure liquid state, is prepared to enter the evaporator [14]. In the evaporator, the low-pressure liquid refrigerant absorbs heat from the environment (e.g., the interior of a refrigerator or a cold storage unit). As it absorbs heat, the refrigerant evaporates and transforms back into a saturated vapor. This phase is critical for the refrigeration

process, as it is responsible for cooling the desired space. The vapor then returns to the compressor, and the cycle repeats [15].

2.2. Performance parameters of the refrigeration system

The collected data is processed and analyzed using thermodynamic equations and performance indicators. Data analysis is performed on all the collected parameters to determine the actual performance of the condenser. This analysis includes the calculation of compressor work, condenser exhaust heat, and refrigeration effect. Additionally, the mass flow rate, actual and ideal COP, and the overall system efficiency are calculated and compared to assess the system's performance before and after optimization. The key parameters related to condenser performance that are measured during the data collection phase are described in the sections below [15].



Figure 3. Condenser of the refrigeration system

2.2.1. Compressor work

Compressor work (W_k) refers to the amount of heat absorbed by the refrigerant per unit mass during the refrigeration process. It is calculated by determining the difference in enthalpy between the inlet and outlet of the compressor. The formula to calculate compressor work is:

$$W_k = h_2 - h_1 \quad (1)$$

where h_1 is the enthalpy at the compressor inlet, and h_2 is the enthalpy at the compressor outlet, both measured in kJ/kg.

2.2.2. Condenser exhaust heat

Condenser exhaust heat represents the amount of heat released by the condenser to the surrounding environment. The condenser unit was shown in Figure 3. It is calculated by subtracting the enthalpy at the condenser outlet from the enthalpy at the condenser inlet. The calculation is based on the following equation:

$$q_c = h_2 - h_3 \quad (2)$$

where h_2 is the enthalpy at the condenser inlet, and h_3 is the enthalpy at the condenser outlet.

2.2.3. Refrigeration effect

The refrigeration effect is the amount of heat that the refrigerant absorbs from the environment or product being cooled. It can be calculated by determining the difference in enthalpy between the outlet and inlet of the evaporator. The equation is:

$$q_k = h_1 - h_4 \quad (3)$$

where h_1 is the enthalpy at the evaporator outlet, and h_4 is the enthalpy at the evaporator inlet, both in kJ/kg.

2.2.4. Refrigerant mass flow rate

The mass flow rate refers to the amount of refrigerant that flows through the refrigeration system per unit time. It can be calculated based on the compressor’s electrical input (voltage and current) and the work done by the compressor. The formula used is:

$$m = \frac{W}{W_k} = V \cdot \frac{I}{1000} / W_{in} \tag{4}$$

where W is the compressor work per unit time (in J/s), W_k is the specific compressor work (in kJ/kg), V is the voltage supplied to the compressor, and I is the current drawn by the compressor (in A).

2.2.5. Coefficient of performance

The actual Coefficient of Performance (COP_{actual}) is a measure of a cooling machine's efficiency. It is calculated as the ratio of the refrigeration effect to the compressor work. The formula is:

$$COP_{actual} : \frac{q_k}{W_k} = \frac{h_1 - h_4}{h_2 - h_1} \tag{5}$$

This helps to quantify how efficiently the system uses energy to transfer heat. Similarly, the ideal Coefficient of Performance (COP_{ideal}) represents the theoretical maximum efficiency of the refrigeration system and is calculated as the ratio of the evaporator temperature to the temperature difference between the condenser and evaporator. This can be expressed as

$$COP_{ideal} : T_e / (T_c - T_e) \tag{6}$$

where T_e is the evaporator inlet temperature, and T_c is the condenser inlet temperature.

2.2.6. Efficiency of refrigeration system

The efficiency of the refrigeration machine is evaluated by comparing the actual COP to the ideal COP. It provides insight into how closely the system operates to its theoretical maximum efficiency. The formula used for this calculation is:

$$n = (COP_{aktual} / COP_{ideal}) \times 100\% \tag{7}$$

3. Results and Discussion

The observation was conducted over a 10-day period, from April 15 to April 24, 2024, on the ammonia refrigeration system installed at the texturizing plant. The data collected during this time represents actual field measurements, providing real-world insights into the system's performance. This data was analyzed in subsequent sections, using the appropriate thermodynamic formulas to evaluate key performance parameters. The analysis will help in understanding the system's behavior under operational conditions and provide a basis for further calculations presented in the following sections.

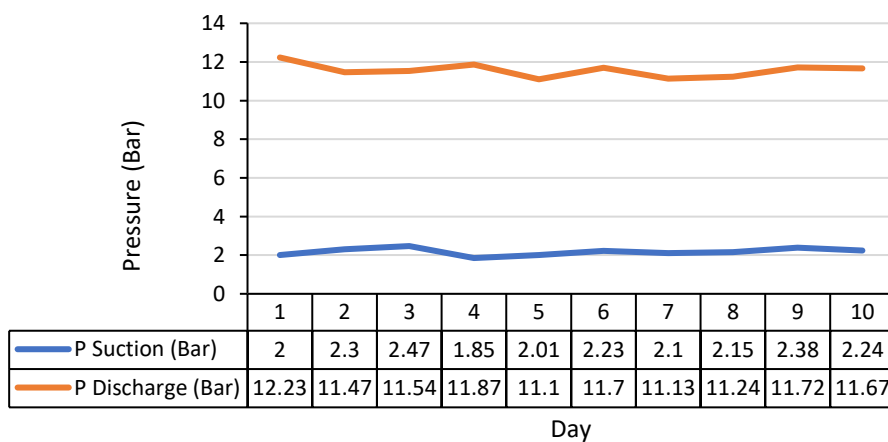


Figure 4. Average compressor suction and discharge pressure

3.1. Actual observation data

The data on Figure 4 present the average compressor suction and discharge pressures measured during the 10-day period. The results show the suction pressure fluctuated between 1.85 and

2.47 bar over the 10 days. The lowest suction pressure was recorded on Day 3 (1.85 bar), while the highest was on Day 3 (2.47 bar). Overall, the suction pressure exhibited minor fluctuations. The discharge pressure ranged between 11.1 and 12.23 bar. The lowest discharge pressure was observed on Day 5 (11.1 bar), while the highest was on Day 1 (12.23 bar). Although the discharge pressure varied slightly throughout the data collection period, it remained within a consistent operational range.

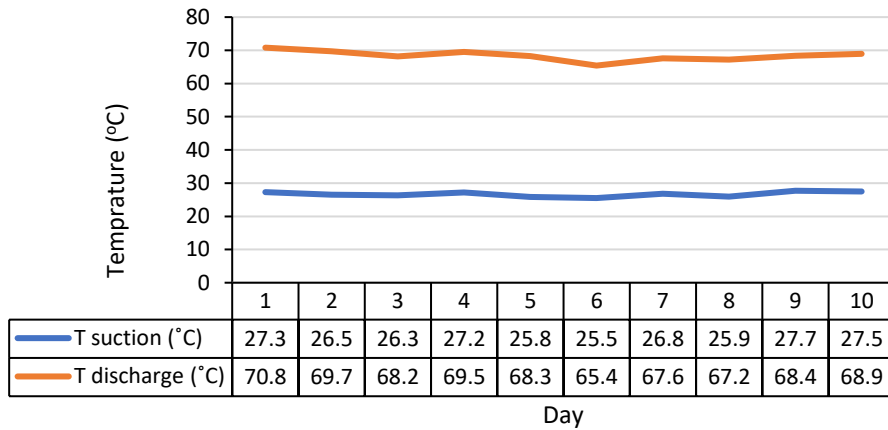


Figure 5. Temperature chart of evaporator inlet and condenser outlet

log(p)-h chart R717 (Ammonia)
 COP (Heat Pump) = 4.39 / COP (Refrigerator) = 3.39

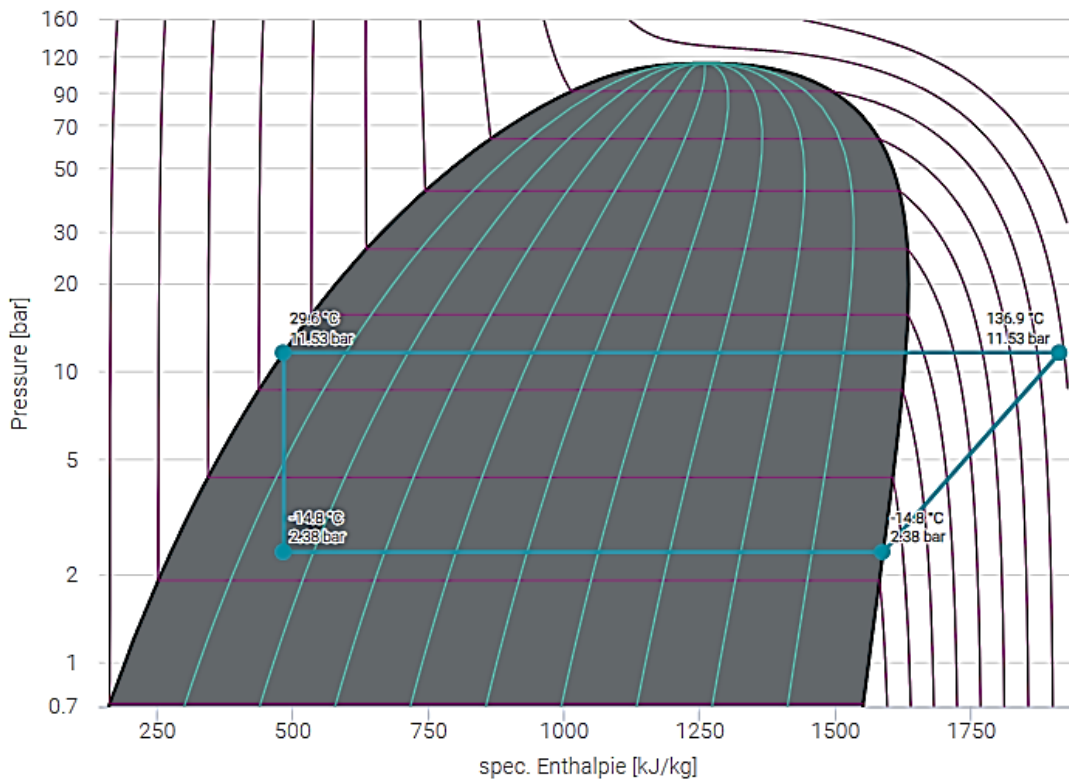


Figure 6. Enthalpy value reading on P-h diagram

To facilitate a clearer understanding of the temperature fluctuations and changes occurring during the data collection process, the average temperature data for the compressor suction and discharge points are presented graphically in Figure 5. The suction temperature remained relatively stable throughout the 10 days, fluctuating between 25.5°C and 27.7°C. The lowest suction temperature was recorded on Day 6 at 25.5°C, while the highest was observed on Day 9 at 27.7°C. These

minor fluctuations indicate consistent refrigerant evaporation at the evaporator, which is essential for maintaining system stability and efficient cooling. The discharge temperature, representing the heat released by the refrigerant after compression, showed more variability, ranging from 65.4°C to 70.8°C. The highest discharge temperature was observed on Day 1 at 70.8°C, while the lowest was recorded on Day 5 at 65.4°C. The fluctuations in discharge temperature reflect the changing heat loads and the ability of the condenser to release heat into the environment.

3.2. Enthalpy of the ammonia refrigerant system

The enthalpy values were calculated by plotting the primary data from field measurements onto the pressure-enthalpy (P-h) diagram for ammonia (R717). This diagram was generated based on the cooling system’s process parameters, including temperature and pressure values observed during the 10-day data collection period.

In the P-h diagram shown above, specific operating points of the ammonia refrigeration cycle were identified and interpreted. For example, the point h2 represents the enthalpy after the compressor (discharge), calculated at 1913.4 kJ/kg, while the point h3 represents the enthalpy at the condenser outlet, which is 482.9 kJ/kg. The enthalpy at point h4, the evaporator outlet, is also 482.9 kJ/kg, indicating a saturated liquid condition at the condenser outlet.

Table 1. Ammonia refrigerant enthalpy value data

Time	Enthalpy value (kJ/kg)		
	h ₁	h ₂	h ₃ = h ₄
15-Apr-24	1588.8	1911.4	486
16-Apr-24	1589.2	1903.4	482.6
17-Apr-24	1586.6	1933.6	491.3
18-Apr-24	1585.3	1935.8	487.3
19-Apr-24	1590	1894.1	479.5
20-Apr-24	1586.4	1923.5	483.9
21-Apr-24	1587.6	1911.7	481.2
22-Apr-24	1588.5	1902.6	479
23-Apr-24	1587.1	1916	481.8
24-Apr-24	1588.1	1900.7	476.1

3.3. Compressor work

Based on the tests conducted, the enthalpy values obtained over the 10-day period were used to calculate the compressor work, following Equation (1). The data presented in the Figure 7 shows the daily compressor work in specific energy (kJ/kg), ranging from 304 kJ/kg to 351 kJ/kg. This graphical representation facilitates a better understanding of the fluctuations in compressor performance throughout the observation period.

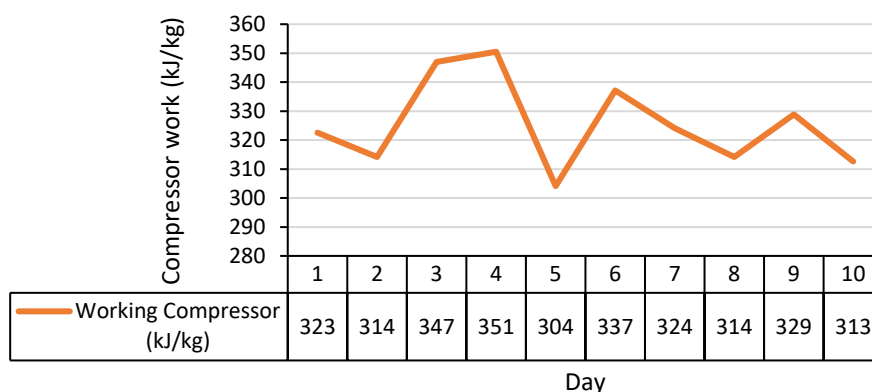


Figure 7. Compressor working chart during data collection

The graph indicates that the compressor work reached its peak on Day 4 at 351 kJ/kg, while the lowest value was recorded on Day 5 at 304 kJ/kg. These fluctuations are linked to the initial temperature of the cooling medium and its influence on the system's overall performance. A lower initial temperature in the cooling medium reduces the energy required for the compressor to operate, as the refrigerant is cooled more efficiently during the condensation process. This results in lower compressor work, as observed on Day 5, where the system likely experienced more favorable cooling conditions. Conversely, when the initial cooling medium temperature is higher, the compressor must exert more energy to achieve the desired cooling effect, leading to an increase in compressor work. This is evident on Day 4, where the compressor work reached its highest value, indicating increased energy demand. The greater the cooling capacity of the refrigerant—directly influenced by the initial temperature of the cooling medium—the less energy the compressor requires to operate. This relationship highlights the importance of optimizing the cooling medium's temperature to minimize compressor work and improve the overall efficiency of the refrigeration system.

3.4. Condenser exhaust heat

The condenser exhaust heat was calculated using the enthalpy values collected over a 10-day period, based on the data provided and calculated using Equation (2). Results from Figure 8 shows that the condenser exhaust heat ranged between 1415 kJ/kg and 1449 kJ/kg during the 10 days of observation. The highest condenser exhaust heat was recorded on Day 4 at 1449 kJ/kg, while the lowest was on Day 5 at 1415 kJ/kg. These variations are influenced by changes in the refrigerant's temperature and the temperature of the cooling medium used in the condenser.

The exhaust heat in the condenser is closely related to the temperature of the cooling medium. When the cooling medium's initial temperature is lower, the condenser operates more efficiently, resulting in an increase in the amount of heat it can dissipate. This can be seen on Days 3 and 4, where the system experienced higher condenser exhaust heat values, likely due to more effective heat transfer conditions. Conversely, when the cooling medium's temperature increases, the condenser's ability to reject heat decreases, as observed on Day 5, where the condenser exhaust heat dropped to its lowest value. The performance of the condenser is significantly affected by the cooling medium's temperature. The lower the cooling medium's initial temperature, the more heat the condenser can release into the environment, leading to improved system efficiency.

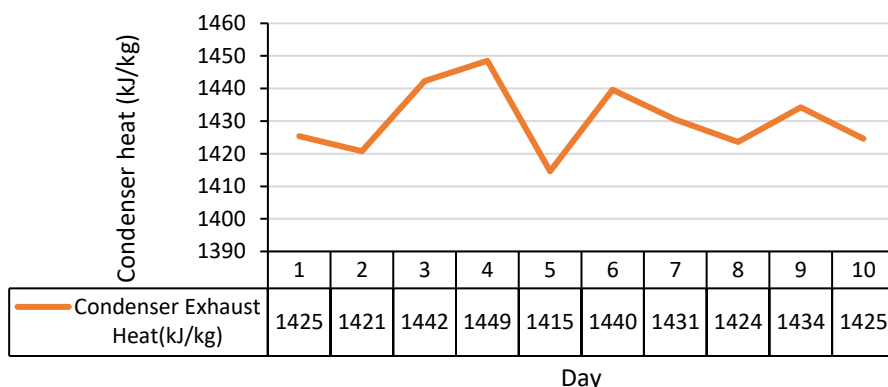


Figure 8. Condenser exhaust heat

3.5. Refrigeration effect

The refrigeration effect was calculated using the enthalpy values collected over the 10-day period, following Equation (3). The results on the Figure 9 shows that the refrigeration effect ranged between 476.1 kJ/kg and 491.3 kJ/kg. The highest value was recorded on Day 3 at 491.3 kJ/kg, while the lowest was observed on Day 10 at 476.1 kJ/kg. These variations can be attributed to changes in the refrigerant temperature and the system's overall heat absorption capacity. When the refrigerant's temperature is lower than the surrounding room temperature, the refrigerant absorbs heat from the environment, which results in a cooling effect. This process causes a decrease in room temperature, and the greater the difference between the refrigerant temperature and the room temperature, the more heat the refrigerant can absorb. This effect is reflected in the higher refrigeration values, such as those seen on Day 3, where optimal conditions allowed for more efficient heat absorption. Conversely, when the temperature difference between the refrigerant and the surrounding environment is smaller, the refrigerant absorbs less heat, leading to a reduced refrigeration effect. This can be

seen on Day 10, where the refrigeration effect reached its lowest value, indicating less effective heat absorption. The refrigeration effect is highly dependent on the temperature difference between the refrigerant and the surrounding environment.

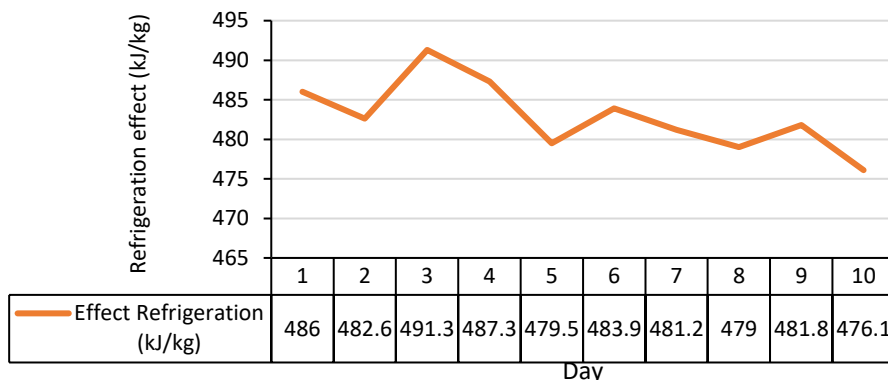


Figure 9. Refrigeration effect

3.6. Refrigerant mass flow rate

Based on testing, it is found that the mass flow rate value for 10 days from the existing data is known to calculate the mass flow rate using Equation (4).

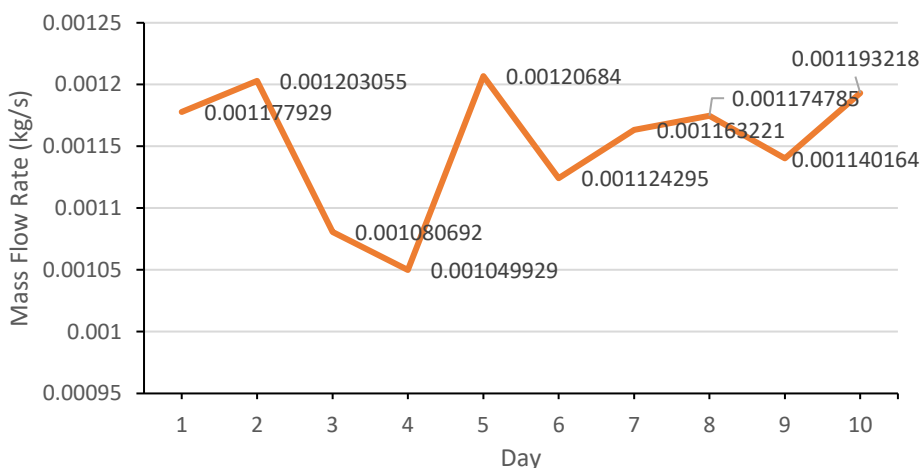


Figure 10. Refrigerant mass flow rate

The mass flow rate of the refrigerant was calculated using the data collected over the 10-day period, following Equation (4). The results on Figure 10 represents the mass flow rate, showing how it fluctuated between 0.001049929 kg/s and 0.001193218 kg/s during the observation period. The highest mass flow rate was recorded on Day 10 at 0.001193218 kg/s, while the lowest value occurred on Day 4 at 0.001049929 kg/s. These variations in mass flow rate are influenced by the refrigerant's ability to transfer heat during the evaporation and condensation processes. When the refrigerant absorbs heat more efficiently, the mass flow rate tends to increase, allowing more refrigerant to flow through the system. This can be observed on Days 5 and 10, where the mass flow rate was higher, indicating more efficient heat transfer and refrigeration processes. The refrigerant mass flow rate is closely tied to the system's ability to transfer heat during the cooling cycle. Higher flow rates are indicative of more efficient heat absorption and release.

3.7. Coefficient of performance

The Coefficient of Performance (COP) for the refrigeration system was calculated over the 10-day period using Equation (5) for actual COP and Equation (6) for ideal COP. The result on Figure 11 shows the actual COP fluctuated between 1.39 and 1.57 over the 10-day period, while the ideal COP remained higher, ranging between 1.69 and 1.84. The gap between the actual and ideal COP indicates the efficiency loss due to real-world factors such as heat loss, friction, and suboptimal

operating conditions. The highest actual COP was observed on Day 5 at 1.57, and the lowest was on Day 4 at 1.39, reflecting variations in system performance due to changing operational parameters such as refrigerant flow rate and cooling medium temperature.

The ideal COP, on the other hand, represents the theoretical maximum efficiency of the system under ideal conditions. It consistently stayed higher than the actual COP, as expected. The ideal COP values in the current study suggest that the system operates below its theoretical efficiency, which is a common observation in practical applications. Similar findings were reported by Terehovics et al. [16], who utilized exergy analysis to evaluate refrigeration systems, highlighting that real-world efficiencies often fall short of ideal values due to various losses in the system. The closer the actual COP is to the ideal COP, the more efficient the refrigeration system is performing. The smallest difference between actual and ideal COP occurred on Day 5, where both values reached their peak performance, indicating that the system operated more efficiently on that day.

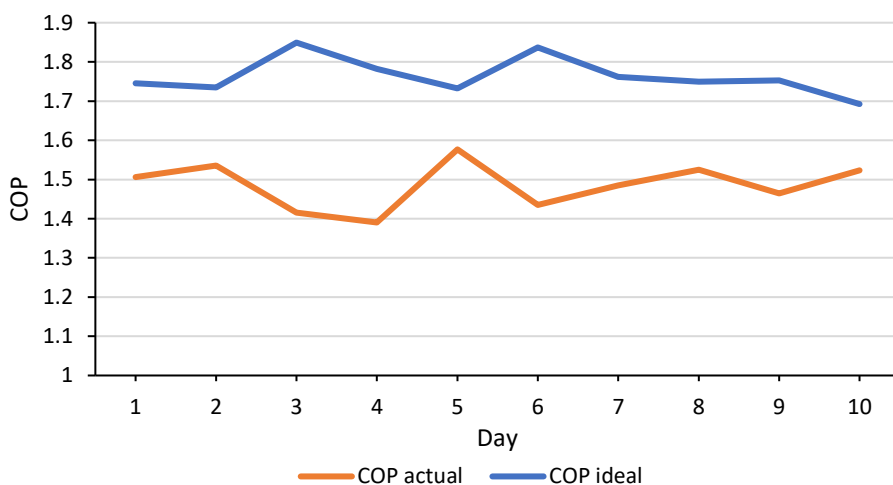


Figure 11. Actual COP actual vs. ideal COP

3.9. System efficiency

The system efficiency over a 10-day period was calculated using Equation (7), and the results are presented in the figure above. The Figure 12 shows the efficiency values ranged from a minimum of 77% on Day 3 to a maximum of 91% on Day 5 align with the findings of Wang et al. [17] who conducted thermodynamic analyses of combined cooling and power systems and noted similar efficiency fluctuations based on varying operational parameters.

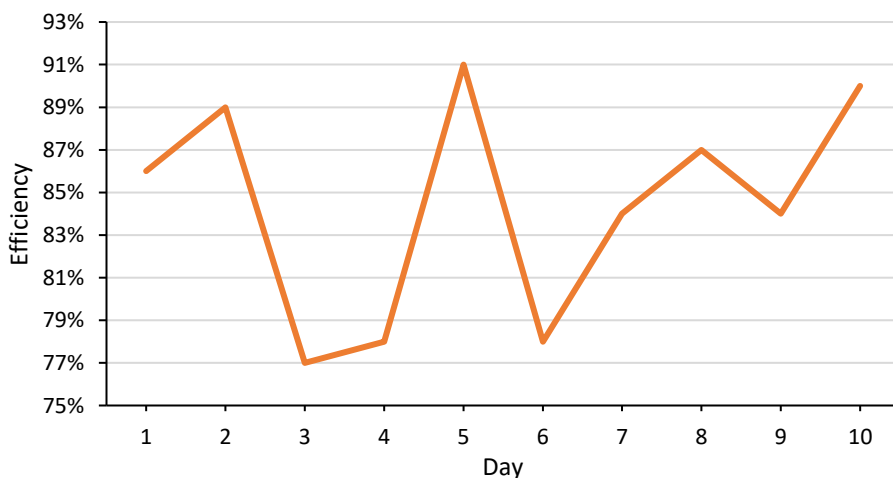


Figure 12. Efficiency of the ammonia refrigeration system

The highest efficiency on Day 5, at 91%, indicates optimal performance of the refrigeration system. This peak can be attributed to the balance of key performance factors such as reduced compressor work, efficient heat rejection in the condenser, and a favorable cooling effect. The system likely experienced better operating conditions on this day, such as lower ambient temperatures or improved heat transfer rates, which contributed to higher overall efficiency. On the other hand, the lowest efficiency, recorded on Day 3 at 77%, suggests a less favorable operating condition. Factors such as increased compressor work, less effective heat rejection from the condenser, or a reduced cooling effect could have contributed to this dip in efficiency. When the cooling medium's temperature or the operational load fluctuates, the system may require more energy to maintain the desired cooling effect, resulting in lower efficiency. Overall, the performance of the refrigeration system is influenced by several factors, including compressor work, condenser exhaust heat, cooling effect, and temperature.

4. Conclusions

In this study, the performance of an ammonia refrigeration system used in a texturizing plant was evaluated over a 10-day period by analyzing key parameters such as compressor work, condenser exhaust heat, refrigeration effect, and system efficiency. The cooling system performed optimally on Day 5, with an efficiency of 91%, while the lowest efficiency, 77%, was observed on Day 3. On Day 5, the system recorded the best performance metrics, with compressor work measured at 304.1 kJ/kg, condenser exhaust heat at 1414.6 kJ/kg, and overall cooling system efficiency at 91%. The highest refrigeration effect was observed on Day 3, with a value of 491.3 kJ/kg, indicating efficient heat absorption on that day despite the lower system efficiency. On Day 4, the system showed a notable mass flow rate of 0.001049929 kg/s, with an actual COP of 1.39. The highest ideal COP value of 1.69 was recorded on Day 10, reflecting theoretical maximum efficiency under ideal conditions. The results indicate that optimizing condenser performance is key to improving overall system efficiency. This can be achieved by controlling temperature and pressure, optimizing airflow or water flow, conducting regular maintenance, and balancing operational loads. When the cooling system operates efficiently, the oil products produced meet the required filling temperature standards. The performance of the ammonia refrigeration system is highly dependent on the efficiency of the condenser. Continuous monitoring of condenser performance is essential, as maximum heat absorption in the condenser leads to higher system efficiency. If the system struggles to reach the target product temperature, actions such as blowing down the condenser and cleaning the condenser basin should be undertaken to enhance heat absorption and maintain system efficiency.

References

- [1] Y. Zhao, Z. Yang, Z. Hou, C. Guo, S. Zhang, and H. He, "Dynamic modeling and leak detection of ammonia leakage in food cold storage system," *J. Food Process Eng.*, vol. 46, no. 12, 2023, doi: 10.1111/jfpe.14483.
- [2] X. Ma and R. Mao, "Fuzzy control of cold storage refrigeration system with dynamic coupling compensation," *J. Control Sci. Eng.*, vol. 2018, pp. 1–7, 2018, doi: 10.1155/2018/6836129.
- [3] J. Wang, P. Zhao, and Y. Dai, "Thermodynamic analysis of a new combined cooling and power system using ammonia–water mixture," *Energy Convers. Manag.*, vol. 117, pp. 335–342, 2016, doi: 10.1016/j.enconman.2016.03.019.
- [4] A. Polzot, P. D'Agaro, P. Gullo, and G. Cortella, "Modelling commercial refrigeration systems coupled with water storage to improve energy efficiency and perform heat recovery," *Int. J. Refrig.*, vol. 69, pp. 313–323, 2016, doi: 10.1016/j.ijrefrig.2016.06.012.
- [5] J. Fitó, A. Coronas, S. Mauran, N. Mazet, and D. Stitou, "Hybrid system combining mechanical compression and thermochemical storage of ammonia vapor for cold production," *Energy Convers. Manag.*, vol. 180, pp. 709–723, 2019, doi: 10.1016/j.enconman.2018.11.019.
- [6] C. Luo, Y. Zhao, and K. Xu, "Study on the regularity of ammonia-related refrigeration accidents in China from 2010 to 2020," *Int. J. Environ. Res. Public Health*, vol. 19, no. 14, p. 8230, 2022, doi: 10.3390/ijerph19148230.
- [7] S. Dharmavaram, M. J. Carroll, E. M. Lutostansky, D. McCormack, A. Chester, and D. Allason, "Red Squirrel tests: air products' ammonia field experiments," *Process Saf. Prog.*, vol. 42, no. 3, pp. 481–498, 2023, doi: 10.1002/prs.12454.
- [8] R. Soujoudi and R. D. Manteufel, "Thermodynamic, economic and environmental analyses of ammonia-based mixed refrigerant for liquefied natural gas pre-cooling cycle," *Processes*, vol. 9, no. 8, p. 1298, 2021, doi: 10.3390/pr9081298.
- [9] M. Sadeghi-Yarandi, M. Mahdini, J. Barzandeh, and A. Soltanzadeh, "Evaluation of the toxic effects of ammonia dispersion," *Med. Gas Res.*, vol. 11, no. 1, pp. 24–29, 2021, doi: 10.4103/2045-9912.310056.
- [10] W. Zhang et al., "Hydrate phase equilibrium data of dimethyl ether in the presence of Tetrahydrofuran, Tetra-n-Butylammonium Bromide, and Cyclopentane," *J. Chem. Eng. Data*, vol. 67, no. 6, pp. 1582–1587, 2022, doi: 10.1021/acs.jced.2c00198.
- [11] R. A. Mahmood, D. Buttsworth, and R. Malpress, "Computational and experimental investigation of using an extractor in the vertical gravitational flash tank separator," *Int. J. Automot. Mech. Eng.*, vol. 16, no. 2, pp. 6706–6722, 2019, doi: 10.15282/ijame.16.2.2019.18.0505.
- [12] P. Kazemiani-Najafabadi, E. A. Rad, and M. Deymi-Dashtebayaz, "Presenting and optimization of a novel ammonia-water combined power and compression cooling system," *Int. J. Energy Res.*, vol. 46, no. 14, pp. 20886–20900, 2022, doi: 10.1002/er.8761.
- [13] H. Caliskan, I. Dincer, and A. Hepbasli, "Thermodynamic analyses and assessments of various thermal energy storage systems for buildings," *Energy Convers. Manag.*, vol. 62, pp. 109–122, 2012.

- [14] D. A. Khudhur, T. A. T. Abdullah, and N. Norazahar, "A review of safety issues and risk assessment of industrial ammonia refrigeration system," *Acs Chem. Heal. Saf.*, vol. 29, no. 5, pp. 394–404, 2022, doi: 10.1021/acs.chas.2c00041.
- [15] Y. A. Cengel, *Thermodynamics: An Engineering Approach*. McGraw-Hill, 2011.
- [16] E. Terehovics, I. Veidenbergs, and D. Blumberga, "Analysis of operation parameters of fish refrigeration by exergy analysis. Case study," *Environ. Clim. Technol.*, vol. 23, no. 1, pp. 229–241, 2019, doi: 10.2478/rtuct-2019-0015.
- [17] H. Wang, J. Wang, Z. Liu, H. Chen, and X. Liu, "Thermodynamic analysis of a new combined cooling and power system coupled by the Kalina cycle and ammonia–water absorption refrigeration cycle," *Sustainability*, vol. 14, no. 20, p. 13260, 2022, doi: 10.3390/su142013260.